Milling Machinability of TiC Particle and TiB Whisker Hybrid Reinforced Titanium Matrix Composites

Huan Haixiang[1,2], *Xu Jiuhua*[1*], *Su Honghua*[1], *Ge Yingfei*[3], *Liang Xinghui*[4]

1. College of Mechanical and Electrical Engineering, Nanjing University of Aeronautics and Astronautics, Nanjing 210016, P. R. China; 2. School of Mechanical Engineering, Yancheng Institute of Technology, Yancheng 224051, P. R. China;
3. School of Mechanical Engineering, Nanjing Institute of Technology, Nanjing 211167, P. R. China;
4. Shanghai Institute of Aerospace Precision Machinery, Shanghai 201600, P. R. China

(Received 23 September 2015; revised 24 December 2015; accepted 28 December 2015)

Abstract: The milling machinabilities of titanium matrix composites were comprehensively evaluated to provide a theoretical basis for cutting parameter determination. Polycrystalline diamond (PCD) tools with different grain sizes and geometries, and carbide tools with and without coatings were used in the experiments. Milling forces, milling temperatures, tool lifetimes, tool wear, and machined surface integrities were investigated. The PCD tool required a primary cutting force 15% smaller than that of the carbide tool, while the uncoated carbide tool required a primary cutting force 10% higher than that of the TiAlN-coated tool. A cutting force of 300 N per millimeter of the cutting edge (300 N/mm) was measured. This caused excessive tool chipping. The cutting temperature of the PCD tool was 20%—30% lower than that of the carbide tool, while that of the TiAlN-coated tool was 12% lower than that of the uncoated carbide tool. The cutting temperatures produced when using water-based cooling and minimal quantity lubrication (MQL) were reduced by 100 °C and 200 °C, compared with those recorded with dry cutting, respectively. In general, the PCD tool lifetimes were 2—3 times longer than the carbide tool lifetimes. The roughness *Ra* of the machined surface was less than 0.6 μm, and the depth of the machined surface hardened layer was in the range of 0.15—0.25 mm for all of the PCD tools before a flank wear land of 0.2 mm was reached. The PCD tool with a 0.8 mm tool nose radius, 0° rake angle, 10° flank angle, and grain size of (30+2) μm exhibited the best cutting performance. For this specific tool, a lifetime of 16 min can be expected.

Key words: titanium matrix composites; milling; machinability; cutting forces; cutting temperature; tool lifetime and tool wear; surface integrity

CLC number: TG506.1 **Document code**: A **Article ID**: 1005-1120(2017)04-0363-09

0 Introduction

As new metal matrix composites, titanium matrix composites (TMCs) have been rapidly developed as replacements for titanium alloys. They have been applied to aeronautics and astronautics, and used in satellite, missile wing, aircraft landing gear, and combustion chamber part applications. However, machining TMCs is challenging because problems such as excessive tool wear, poor surface finish, and low productivity are often encountered. Machining accounts for more than 60% of the total TMC part production cost. This severely restricts their use in a variety of applications[1-4]. Therefore, it is important to reduce TMC machining costs by studying their machinabilities. However, investigations of TMC machining are still in their early stages despite several published articles addressing the issue. Earlier studies showed that high speed steel tools are unsuitable for cutting TMCs and that carbide tools can be used only for rough machining, with very

* Corresponding author, E-mail address: jhxu@nuaa.edu.cn.

How to cite this article: Huan Haixiang, Xu Jiuhua, Su Honghua, et al. Milling machinability of TiC particle and TiB whisker hybrid reinforced titanium matrix composites[J]. Trans. Nanjing Univ. Aero. Astro., 2017,34(4):363-371.
http://dx.doi.org/10.16356/j.1005-1120.2017.04.363

short tool lives (2—5 min)[5-8]. Polycrystalline diamond (PCD) tools are also used to turn this type of difficult-to-machine material with the aid of laser heating[9]. Laser assisted machining (LAM) can increase tool life by up to 180% when working with 10—12 vol% of particles reinforced Ti-6Al-4V matrix composites. The surface roughness increased by up to 15%, tool diffusion wear increased, and tool lifetime decreased when high cutting speeds and high laser power were applied. Unfortunately, despite its importance, investigations of TMC milling machinability have not been performed until now. To better understand the related milling problems, the influences of tool materials, tool geometries, tool grain sizes, and cooling conditions on the cutting forces, cutting temperature, tool lifetimes, and machined surface quality are studied, and tool wear mechanisms are analyzed. The objective of this study is to provide a theoretical basis for the practical selection of cutting parameters.

1 Experimental Materials and Procedures

Titanium carbide particles and titanium boride whisker hybrid reinforced titanium matrix composites with a reinforcement volume fraction of 10% were adopted as the workpiece materials (10% by volume (TiC_p + TiB_w)/Ti-6Al-4V). The titanium carbide particle diameters ranged from 1.5 μm to 20 μm and the titanium boride whisker lengths varied from 35 μm to 80 μm (Fig. 1).

Carbide tools and Supower™ PCD inserts with grain sizes of 10, 25, and (30+2) μm were used in the tests. The cutting tool details are listed in Table 1. The milling tests were performed using an MIKRON UCP710 high-speed five-axis vertical machine center in down milling mode[10].

The cutting parameters were: cutting speed of 100 m/min, feed rate of 0.08 mm/tooth, radial cut depth of 1 mm, and axial cut depth of 3 mm. During dry cutting, a water-based coolant, and minimum quantity lubrication (MQL) were tested.

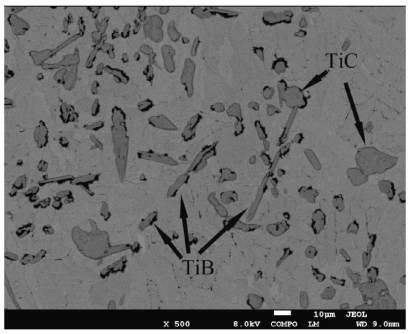

Fig. 1 Microstructure of a (TiC_p + TiB_w)/Ti-6Al-4V composite with 10 vol% particulate matter

A Kistler 9272 piezoelectric dynamometer and the associated 5019A charge amplifier were used to measure the three components of the cutting force. $\boldsymbol{F}_x$, $\boldsymbol{F}_y$, and $\boldsymbol{F}_z$ represent the force in the feed direction/main cutting force and the forces in the radial and axial directions, respectively.

Table 1 Details of the cutting tools used in experiments

Tool number	Tool composition	Tool grain size/μm	Flank angle/(°)	Rake angle/(°)	Trimming edge	Tool nose radius/mm	Coating
1	PCD	10	15	0	No	0.4	No
2	PCD	10	15	0	No	0.8	No
3	PCD	25	10	8	Yes	0.8	No
4	PCD	25	10	0	Yes	0.8	No
5	PCD	25	10	0	No	0.8	No
6	PCD	30+2	10	0	Yes	0.8	No
7	PCD	30+2	10	0	No	0.8	No
8	PCD	10	10	0	No	0.8	No
9	Carbide WMG40	0.5—2.0	20	25	Yes	0.8	No
10	Carbide WXN15	0.5—1.0	20	25	Yes	0.8	TiAlN

A constantan thermocouple was used to measure the workpiece milling temperature. As shown in Fig. 2, a hot junction was formed with the thermocouple when the tool cut the constantan and the workpiece material, while the cold junction was far from the cutting zone. The electric potential signal generated between the hot and cold thermocouple junctions was recorded using an NI USB-6211 multi-functional signal ac-

quisition system. The cutting temperature could be calculated from the electric potential of the workpiece-constantan thermocouple pair after calibration with a special calibration system (Fig. 3). This calibration was performed using a standard NiCr-NiSi thermocouple. Both thermocouples shared a hot junction to ensure that they sensed the same temperature during calibration. The cold junctions of both thermocouples were maintained at room temperature. The temperature differences between the hot and cold junctions were determined by measuring the corresponding electric potentials. The electric potential-temperature graph shown in Fig. 4 was plotted after measuring several different temperature/electric potential pairs. That is to say, the temperature can be determined based on any electric potential measurement. The correlation associated with the electric potential-temperature graph shown in Fig. 4 is

$$Y = 3.077\ 8 + 26.086X - 0.278\ 5X^2 + 0.002\ 1X^3 \quad (1)$$

where Y is the cutting temperature (°C) and X the electric potential (mV).

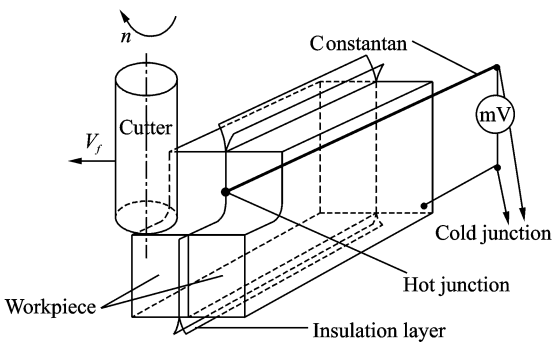

Fig. 2 Cutting temperature measurement during TMC milling

A Hirox KH-7700 three-dimensional video microscope was used to capture and measure tool wear on the flank. Failure was assumed when the flank wear land measurement (VB) was larger than 0.2 mm. Tool wear was observed using a scanning electron microscope (SEM, Hitachi S-3400).

Surface roughness and micro hardness were used to evaluate the machined surface quality.

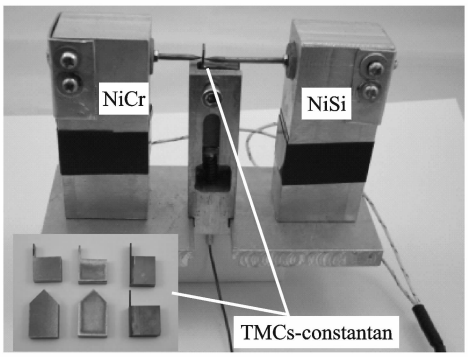

Fig. 3 Apparatus and calibration samples

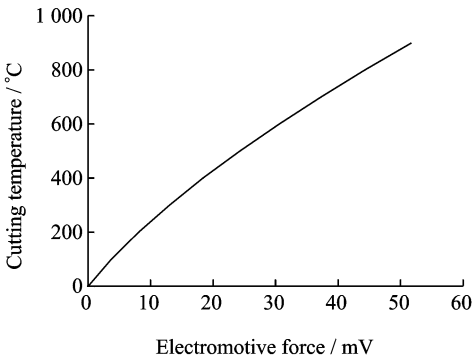

Fig. 4 Calibration curve for (TiC_p + TiB_w)/Ti-6Al-4V-constantan thermocouple

The surface roughness was measured in the tool feed direction using a Mahr Perthometer M1 surface analysis instrument. The cut-off length was set to 17.5 mm. Hardness tests were conducted using a HXS-1000A (Shanghai BM optical instruments) micro hardness testing unit with a load of 100 g and 15 s time delay.

2 Results and Discussion

2.1 Cutting forces

Fig. 5 shows the cutting forces applied by the PCD (No. 6) and carbide tools WMG40 (No. 9) and WXN15 (No. 10). The main cutting force applied by the PCD tool is 780 N, which is 15% less than the one required of the carbide tools, even though the rake and flank angles of the carbide tools are higher than those of the PCD tool. This may be because the friction coefficient between carbide and the TMCs is significantly higher than that between PCD and the TMCs. In addition, the carbide-TMC affinity is much stronger than

the PCD-TMC affinity[11-12]. Fig. 5 also shows that the main cutting force F_x associated with the uncoated WMG40 tool is 940 N, which is 10% higher than that of the TiAlN-coated WXN15 tool.

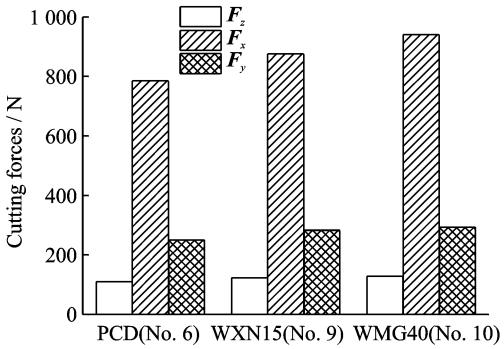

Fig. 5 Cutting force by tool material (water-based cooling)

2.2 Cutting temperature

Tools No. 7, 8 (PCD tools) and No. 9, 10 (carbide tools) were used to investigate the influences of the tool composition and tool grain size on cutting temperature. As seen in Fig. 6, the cutting temperatures produced by the PCD tool with (30+2) μm grains and the tool with 10 μm grains are nearly identical (305 °C). This implies that the grain size has little effect on the cutting temperature. However, the tool composition influences the cutting temperature significantly. As seen in Fig. 6, the cutting temperature for the uncoated carbide tool is 460 °C, which is 15% and 43% higher than that for the TiAlN-coated carbide tool and the PCD tool, respectively. This result is attributed to the lower PCD friction coefficient and higher thermal diffusivity of TiAlN (the thermal diffusivity of the TiAlN coating is 4.5 times higher than that of the carbide matrix)[13-14].

In addition to the effect of the tool material, cooling conditions significantly influence the cutting temperature. Fig. 7 shows the effect of dry cutting, as well as use of a water-based coolant and MQL on the cutting temperature. The cutting temperatures produced using the MQL and water-based coolant are 100 °C and 200 °C lower, respectively, than those produced during dry cutting. Therefore, either the water-based coolant or MQL can reduce the cutting temperature effectively. However, the water-based coolant is better. Fig. 7 also shows that the presence of a trimming edge has no effect on the cutting temperature.

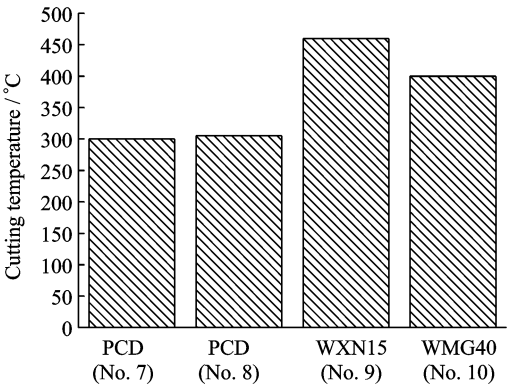

Fig. 6 Cutting temperature by tool material (water-based cooling)

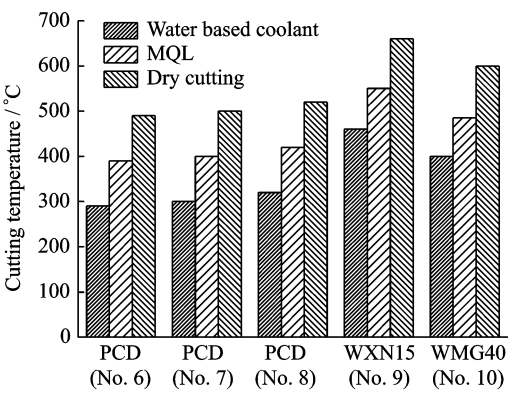

Fig. 7 Effect of cooling conditions and tool material on cutting temperature

2.3 Tool life

Tool No. 1 through No. 4 and NO. 8 was used to study the effects of tool nose radius, rake angle, and flank angle on tool lifetime. The results are shown in Fig. 8. The wear rate of tool No. 1 (tool nose radius=0.4 mm) was 1.3 times higher than that of tool No. 2 (tool nose radius r=0.8 mm). By comparing the tool lifetime graphs of tools No. 3 (rake angle=8°) and No. 4 (rake angle=0°) (Fig. 8), it can be seen that the lifetime obtained with the larger rake angle is only 1/3 of that obtained with a smaller rake angle. By studying the tool lifetime graphs of No. 2 (flank angle=15°) and No. 10 (flank angle=10°) in Fig. 8, it is observed that the latter lasts 1.3

times longer than the former. Based on the above results, it is inferred that larger nose radius and smaller rake or flank angles provide longer tool lifetimes.

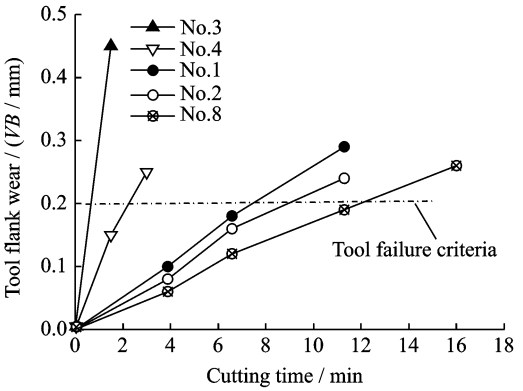

Fig. 8 Effects of PCD tool geometries on tool lifetime (water-based cooling)

To investigate the effect of tool grain size on lifetime, tools No. 5 through No. 8 were used to mill TMCs. The graphs of flank wear (VB) versus cutting time are shown in Fig. 9. Under identical cutting conditions, the tool with 25 μm grains (No. 5) failed after cutting only for 2 min while tools with grain sizes of (30+2) μm (Nos. 6, 7) and of 10 μm (No. 8) performed well for 15, 16, and 11 min, respectively. Thus, the tool with a grain size of (30+2) μm exhibited the longest lifetime. Fig. 9 also shows that the presence of a trimming edge has no effect on tool lifetime.

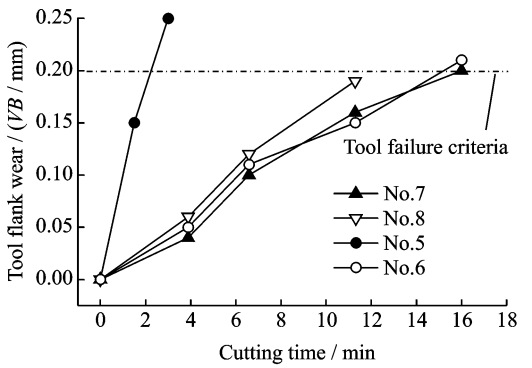

Fig. 9 Effect of PCD grain size and presence of a trimming edge on tool lifetime (water-based cooling)

Fig. 10 shows the lifetimes of PCD and carbide tools. The lifetimes of the PCD tools are 2—3 times longer than those of the carbide tools. This is because the hardness and thermal conductivity of PCD are higher than those of carbide by cutting force 80—120 times and 9 times, respectively[15-16]. Therefore, the cutting force and temperature associated with the PCD tools are significantly lower than those produced by the carbide tools (see Sections 2.1, 2.2).

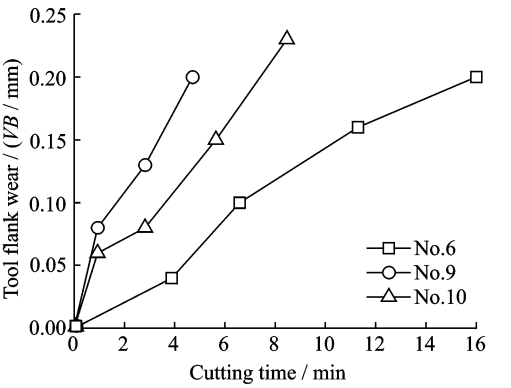

Fig. 10 PCD and carbide tool lifetimes (water-based cooling)

2.4 Tool wear mechanisms

With the PCD tools, the primary mechanisms of tool wear and damage during TMC milling are abrasive wear, chipping, and detachment of the tool material (the PCD grain or the adhesive).

Typically, the PCD tool exhibits chipping or micro-chipping during TMC milling. Fig. 11 shows the typical appearance of a chipped tool. There are two causes of PCD tool chipping during TMC milling. One is the relatively low impact resistance of PCD, while the other is the very high specific cutting force on the cutting edge. In Fig. 5, the cutting force reaches 300 N/mm. Thus, the material removal rate should be minimized during TMC milling in order to improve the tool lifetime.

An example of material detachment from a PCD tool is shown in Fig. 12. Two types of material detachment have been observed. The first is plucking of diamond grains (from the PCD tool), which is induced by the abrasive effects of hard phases in the TMCs. The fine grooves on the

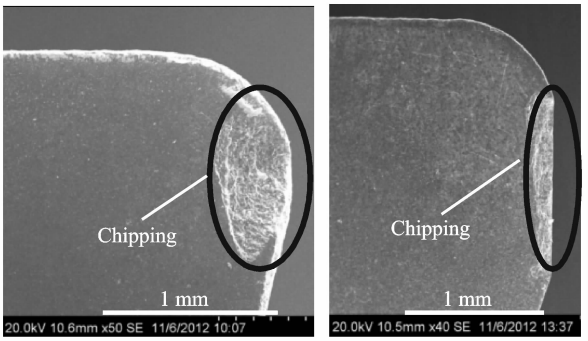

(a) No.5 tool (b) No.4 tool

Fig. 11 Typical appearance of chipped PCD tools (used in milling for 1 min with water-based cooling)

(a) Flank face

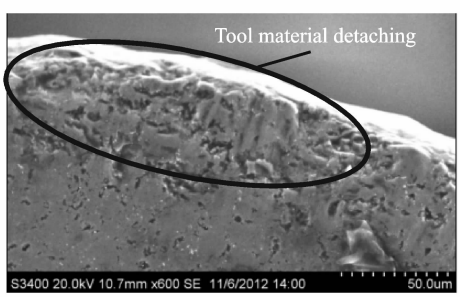

(b) Rake face

Fig. 12 Typical detached PCD tool materials (No. 6, used in milling for 11 min with water-based cooling)

flank face shown in Fig. 12(a), result from abrasive wear. The other mechanism of detachment is the loss of a piece of tool material (PCD grain and binding material), caused by adhesive wear. Smearing and pitting on the rake face, which are side effects of adhesive wear, are also shown in Fig. 12(b). When milling the TMCs with a PCD tool, the cutting force and temperature are high (see Sections 3.1 and 3.2) and work hardening can easily take place in the titanium matrix. Accordingly, a build-up edge forms on the tool face (Fig. 13). Detachment causes the loss of tool material or adhesive wear.

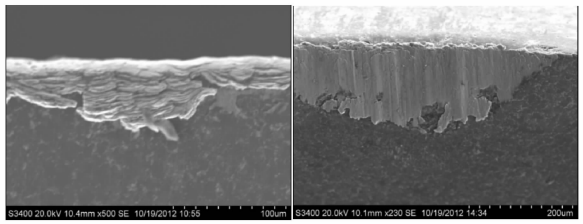

(a) Rake face (b) Flank face

Fig. 13 Typical appearance of Ti matrix materials adhered to a PCD tool (water-based cooling)

In addition to the chipping and abrasive wear observed with PCD tools, the carbide tools often exhibit micro-cracks and significant amounts of peeling. Cracks due to mechanical (Fig. 14(a)) and thermal fatigue (Fig. 14(b)) occur on the tool nose when the carbide tools are etched and ultrasonically cleaned after cutting. Generally, mechanical fatigue cracks manifest parallel to the tool nose while thermal fatigue cracks appear perpendicular to the cutting edge on the tool nose. Mechanical fatigue cracks are caused primarily by interruptions in cutting and load fluctuations while thermal fatigue cracks are induced by periodic thermal expansion and contraction during milling[17].

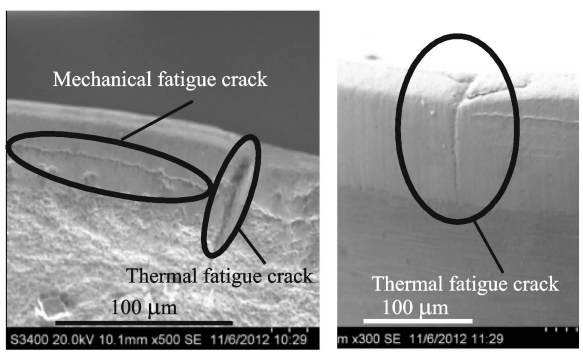

(a) No. 10 after 8.5 min of cutting (b) No. 9 after 4.7 min of cutting

Fig. 14 Two types of micro-cracks on carbide tools after milling (TiC_p + TiB_w)/Ti-6Al-4V with water-based cooling

The TiAlN-coated carbide tool (No. 10) can also exhibit severe coating material peeling, as shown in Fig. 15. This peeling occurs due to mechanical and thermal stresses and unequal expan-

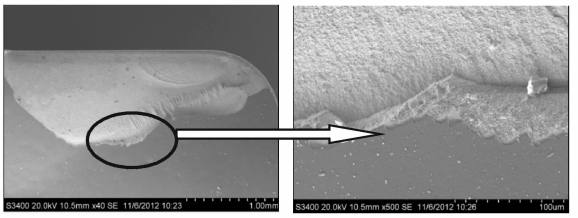

Fig. 15 Typical peeling of TiAlN coating from a carbide tool (after milling for 8.5 min with water-based cooling)

sion of the coating material and carbide matrix due to differences in their thermal expansion coefficients.

2.5 Machined surface integrity

2.5.1 Surface roughness

Fig. 16 shows the roughnesses of the machined surfaces obtained after milling using PCD tools with varying grain sizes. The tool with 10 μm grains produces the lowest surface roughness ($Ra=0.28$ μm), followed by the tool with (30+2) μm grains ($Ra=0.37$ μm). The tool with 25 μm grains produces the highest surface roughness ($Ra=0.42$ μm). Thus, the tool grain size has a significant effect on the machined surface roughness. Generally, smaller tool grain sizes produce lower machined surface roughnesses.

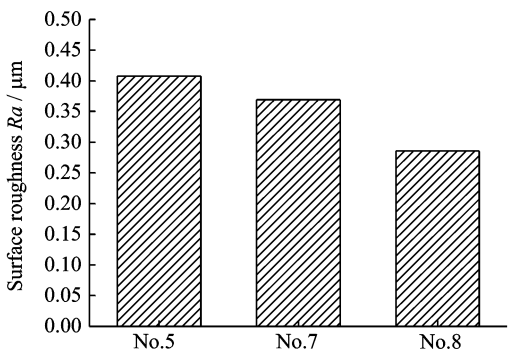

Fig. 16 Effect of PCD grain size on machined surface roughness (water-based cooling)

Fig. 17 shows the variation in machined surface roughness with tool wear. The surface roughness increases slowly (by 8%) when the tool is in its initial stage of wear ($VB\sim0$—0.1 mm). However, the surface roughness increases dramatically (by 30%) as the tool wear increases when the VB is higher than 0.1 mm. However, the surface roughness is less than $Ra=0.55$ μm when the tool wear reaches the failure criterion ($VB=0.2$ mm).

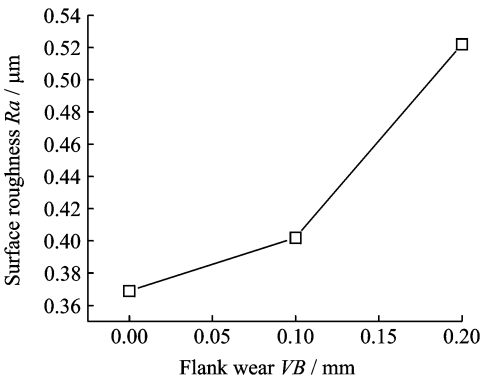

Fig. 17 Effect of tool wear on machined surface roughness (water-based cooling)

2.5.2 Machined surface and subsurface microhardness

Fig. 18 shows that the depth of the deformation hardening layer of a new tool is 0.19 mm, and that the average micro hardness of the deformation layer is 375 HV. When the tool wear increases to VB of 0.2 mm, the depth of the deformation hardening layer increases by 40% to 0.27 mm and the average micro hardness of the deformation layer reaches 395 HV. If higher cutting speed is used, a soft layer is presented when the tool is worn out. As shown in Fig. 19, a soft layer 0.12 mm in depth is found when a cutting speed of 200 m/min is used and VB 0.2 mm is reached.

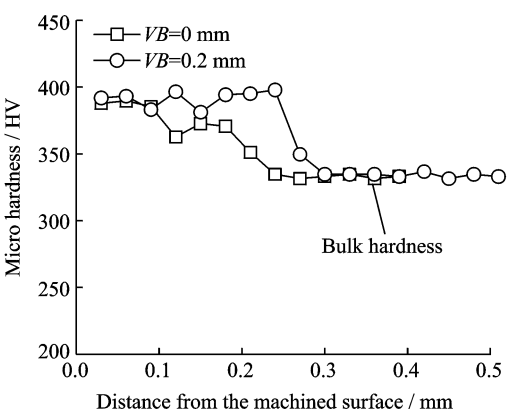

Fig. 18 Effect of tool wear on micro hardnesses of the machined surface and subsurface (tool No. 6 with water-based cooling)

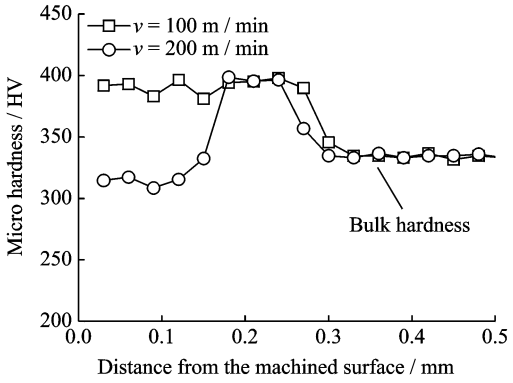

Fig. 19 Effect of cutting speed on micro hardnesses of the machined surface and subsurface (VB = 0.2 mm, water-based cooling)

3 Conclusions

(1) The PCD tool clearly outperformed the carbide tool in TMC milling. Under the selected cutting conditions, the main cutting force exerted by the PCD tool was 780 N, which was 15% less than required for the carbide tool. The PCD tool life was 2—3 times longer than that of the carbide tool. The PCD tool cutting temperature was generally 20%—30% lower than that of the carbide tool. The cutting force and temperature of the uncoated carbide tool were 10% and 15% higher, respectively, than those of the TiAlN-coated carbide tool. With the PCD tool, the cutting force per unit length of the cutting edge was 300 N/mm. The presence of such a large cutting force was one reason for tool chipping.

(2) The PCD grain size and presence of a trimming edge had weak effects on the cutting force and temperature. The cutting force had a significant effect on tool lifetime. Tools with larger nose radius along with smaller rake angles, flank angles, and grain sizes exhibited significantly improved tool lifetimes. With PCD tools, the main mechanisms of wear and damage were abrasive wear, chipping, and tool material detachment. In carbide tools, cracking from mechanical and thermal fatigue and excessive coating material peeling provided additional failure mechanisms.

(3) Under dry cutting conditions, the PCD tools operated at cutting temperatures of 500—550 °C. With water-based cooling and minimum quantity lubrication, the cutting temperature decreased by 100 °C and 200 °C, respectively.

(4) The machined surface roughness of the PCD tool was less than $Ra = 0.55$ μm before the flank wear VB exceeded 0.2 mm. For all of the PCD tools tested at a cutting speed of 100 m/min, the depth of the machined, surface-hardened layer remained in the range of 0.15—0.25 mm before reaching the tool failure criterion. A soft layer 0.12 mm in depth was formed when milling was performed with a worn tool and a cutting speed of 200 m/min.

(5) The PCD tool with a 0.8 mm tool nose radius, 0° rake angle, 10° flank angle, and grain size of (30+2) μm exhibited the best cutting performance. The expected lifetime of this tool is 16 min.

Acknowledgments

This work was supported by the National Natural Science Foundation of China (No. 51275227), the Funding of Jiangsu Innovation Program for Graduate Education (No. CXLX11_0175), and the Shanghai Aerospace Science and Technology Innovation Fund (No. SAST201326).

References:

[1] ABKOWITZ S, ABKOWITZ S M, FISHER H, et al. CermeTi® discontinuously reinforced Ti-matrix composites: Manufacturing, properties and applications[J]. JOM, 2004,56(5):37-41.

[2] CHEN X Q, LIU X T. Aeronautical engineering materials[M]. Beijing: AIP, 2008. (in Chinese)

[3] LIN Z W, LIU Y Q, LIANG Y, et al. Application of carbon fiber reinforced composite to space optical structure[J]. Opt Precision Eng, 2007,15(8):1181-1185. (in Chinese)

[4] CHEN L F. Study on the in-situ generated powder metallurgy titanium matrix composites[D]. Changsha: Central South University, 2005:1-8. (in Chinese)

[5] HAYERS S M, AMULU M, PEDESEN W E. Machining characteristics of a titanium metal matrix composite[C]//The 29th North American Manufacturing Research Conference. Florida, USA: [s. n.], 2001.

[6] GE Y F, XU J H, FU Y C. High-speed turning of titanium matrix composites with PCD and carbide tools[J]. Mater Sci Forum, 2014,770:39-44.

[7] ARAMESH M, SHI B, NASSEF A O, et al. Meta-modeling optimization of the cutting process during turning titanium metal matrix composites (Ti-MMCs)[J]. Procedia CIRP, 2013,8:576-581.

[8] ARAMESH M, SHABAN Y, BALAZINSKI M, et al. Survival life analysis of the cutting tools during turning titanium metal matrix composites (Ti-MMCs)[J]. Procedia CIRP, 2014,14:605-609.

[9] BEJJANI R, SHI B. Laser assisted turning of titanium metal matrix composite[J]. CIRP Ann-Manuf Techn, 2011,60:61-64.

[10] YING G F, CHEN Y, FU Y C, et al. Cutting force in face milling of milling of Invar36 alloy[J]. J Nanjing Univ Aeronaut Astronaut, 2014, 46(5): 713-719. (in Chinese)

[11] WEI W H. Basic research on improving the machinability of titanium alloy by hydrogen treatment[D]. Nanjing: Nanjing University of Aeronautics & Astronautics, 2010:71-81. (in Chinese)

[12] PARK K H, BEAL A, KIM D, et al. Tool wear in drilling of composite/titanium stacks using carbide and polycrystalline diamond tools[J]. Wear, 2011, 271:2826-2835.

[13] KRISHNARAJ V, SAMSUDEENSADHAM S, SINDHUMATHI R, et al. A study on high speed end milling of titanium alloy[J]. Procedia Eng, 2014,97:251-257.

[14] DEIAB I, RAZA S W, PERVAIZ S. Analysis of lubrication strategies for sustainable machining during turning of titanium Ti-6Al-4V alloy[J]. Procedia CIRP, 2014,17:766-771.

[15] ZEBALA W, KOWALCZYK R, MATARAS A. Analysis and optimization of sintered carbides turning with PCD tools[J]. Procedia Eng, 2015,100:283-290.

[16] AMIN A K M N, ISMAIL A F, KHAIRUSSHIM M K N. Effectiveness of uncoated WC-Co and PCD inserts in end milling of titanium alloy—Ti-6Al-4V[J]. J Mater Process Technol, 2007(192/193):147-158.

[17] WEI W H, XU J H, FU Y C, et al. Study on the machinability of titanium alloy TC4 produced by the method of hydrogen treatment[J]. J Nanjing Univ Aeronaut Astronaut, 2009,41(5):633-638. (in Chinese)

Mr. **Huan Haixiang** is a Ph. D. candidate of Nanjing University of Aeronautics and Astronautics (NUAA). He received his M. S. degree in mechanical engineering from Jiangsu University, China, in 2007. His research interests focus on high-performance machining of metal matrix composites.

Prof. **Xu Jiuhua** is a professor and Ph. D. advisor in the College of Mechanical and Electrical Engineering at NUAA. His research interests focus on fabrication of diamond and CBN super-abrasive tools, green manufacture, and machining technology for difficult-to-cut materials.

Prof. **Su Honghua** is a professor and Ph. D. superivor in the College of Mechanical and Electrical Engineering at NUAA in China. His research interests focus on cutting, grinding-for difficult-to-cut materials, etc.

Dr. **Ge Yingfei** is an associate professor in Nanjing Institute of Technology. He received his Ph. D. degree in mechanical engineering from NUAA, China, in 2007. His research interests focus on high-performance machiningof difficult-to-cut materials.

Ms. **Liang Xinghui** is a senior engineer in Shanghai Institute of Aerospace Precision Machiner. She received her M. S. degreein mechanical engineering from NUAA, China, in 2012. Her research interests focus on high speed machining of difficult-to-cut materials.

(Executive Editor: Zhang Tong)